

# Superlattices of Metal and Metal–Semiconductor Quantum Dots Obtained by Layer-by-Layer Deposition of Nanoparticle Arrays

K. Vijaya Sarathy, P. John Thomas, G. U. Kulkarni, and C. N. R. Rao\*

Chemistry and Physics of Materials Unit, Jawaharlal Nehru Centre for Advanced Scientific Research, Jakkur, Bangalore-560 064, India

Received: September 23, 1998; In Final Form: November 12, 1998

Superlattices formed by arrays of Pt or Au nanoparticles have been obtained by layer-by-layer deposition by using dithiols as cross-linkers. The superlattices have been characterized by X-ray diffraction, photoelectron spectroscopy, and scanning tunneling microscopy. The core-level intensities of the metal and of the dithiol in the X-ray photoelectron spectra show the expected increase with successive depositions. The formation of such structures has been confirmed by depositing Pt and Au layers alternatively. Layers of metal and CdS nanoparticles have been deposited alternatively to obtain heterostructures.

The quest for nanoscale architectures has provided much impetus to investigate the self-assembly of metal and semiconductor particles as well as of other materials. A major motivation to construct such structures has been to exploit the novel properties that would manifest from size quantization which may allow band-gap engineering and to design nanoelectronic devices, sensors, and the like. Thus, Colvin et al.<sup>1</sup> have made use of a self-assembly of semiconductor nanocrystals to construct an optoelectronic device. Murray et al.<sup>2</sup> have demonstrated the self-organization of CdSe nanocrystallites into a three-dimensional superlattice. Multilayers of semiconductor CdS nanoparticles have been deposited on a gold substrate using the self-assembly of dithiol molecules.<sup>3,4</sup> There has been some effort to obtain regular arrangements of metal nanoparticles in different dimensions. A linear arrangement of Au clusters stabilized by phosphine ligands has been obtained by binding them to single-stranded DNA,<sup>5</sup> while ordered channels of porous alumina membranes have been filled with Au particles to obtain wires.<sup>6</sup> Two-dimensional arrays of metal nanoparticles are readily prepared by using alkanethiols.<sup>7–9</sup> Whetten et al.<sup>9</sup> have described gold nanocrystals stabilized by thiols. Although there are indications that multilayers of metal particles can be formed by use of dithiols,<sup>4</sup> there is no definitive evidence, based on spectroscopic, microscopic, and diffraction studies, for such superstructures. It was our interest to prepare superlattices of well-characterized metal quantum dots by use of spacer molecules. In this letter, we report the layer-by-layer deposition of nanocrystalline arrays of quantum dots of a single metal or of two metals by employing dithiol molecules to construct superlattices. Such lattices with alternate layers of metal and semiconductor nanoparticles can also be prepared.

The procedure employed to obtain metal quantum dot superlattices is simple. A clean polycrystalline metal substrate of gold or silver, prepared by the resistive evaporation of the metal onto a freshly cleaved mica substrate at 500 °C in a vacuum, was immersed in a 50 mM toluene solution of 1,10-decanedithiol. After 2 h, it was washed with toluene and dried in air. The dithiol-covered substrate was then immersed in a dilute dispersion of metal nanoparticles of the desired size (obtained by the controlled reduction of metal ions complexed

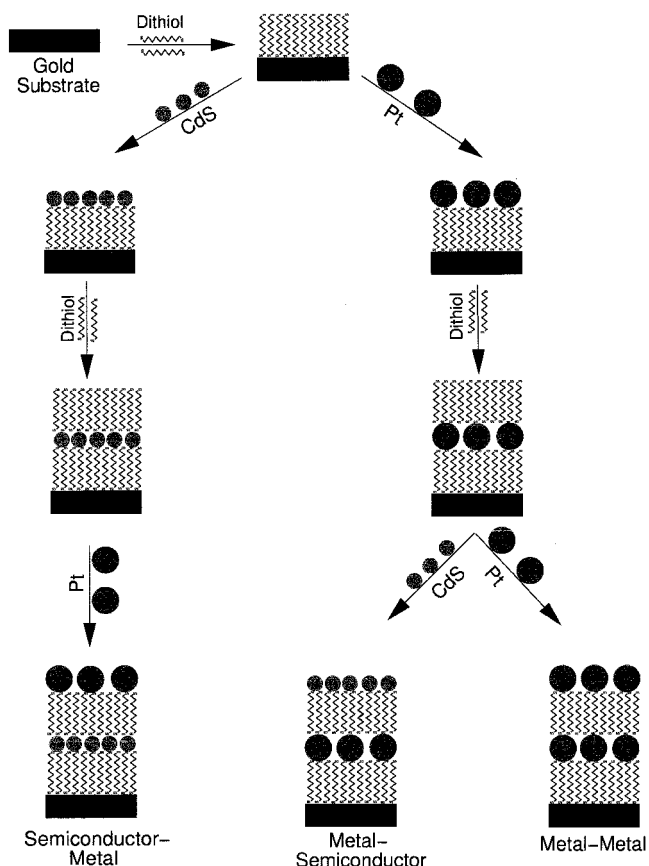


**Figure 1.** Schematic drawing depicting the layer-by-layer deposition of Pt nanoparticles onto a Au substrate, the layers being separated by dithiol molecules. Also shown is the formation of a heterostructure consisting of alternate layers of semiconductor and metal nanoparticles.

with tetra-*n*-octylammonium bromide in toluene using NaBH<sub>4</sub>) in toluene for 12 h. After the formation of a particulate layer by this means, it was washed with toluene and dried. The above steps employed for depositing the first layer of nanoparticles were repeated to obtain multilayer superlattices. This is shown schematically in Figure 1. After each deposition, the nanostructures were characterized by X-ray and UV photoelectron spectroscopy (XPS and UPS), scanning tunneling microscopy

\* Corresponding author.

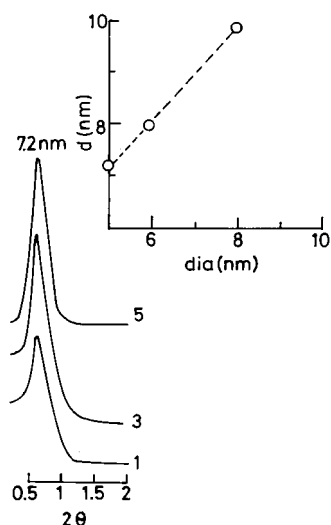


**Figure 2.** X-ray diffraction patterns of nanocrystalline arrays of the 5 nm Pt particles on a Au substrate after the first, third, and fifth depositions. The inset shows the variation in the  $d$ -spacing due to nanocrystalline arrays formed by the particles of different diameters. Layers of 1.5 nm Pt particles did not give a XRD pattern.

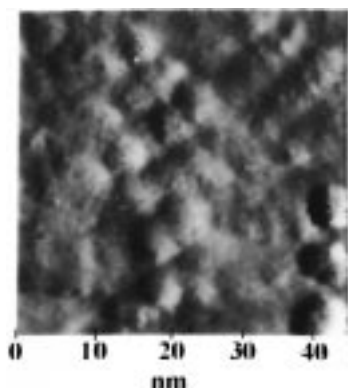


**Figure 3.** Scanning tunneling image of the first layer of the 5 nm Pt particles on a Au substrate.

(STM), and X-ray diffraction (XRD). The metal nanoparticles employed were characterized by transmission electron microscopy (TEM) to determine the size distribution.

In Figure 2, we show typical XRD patterns of lattices formed by Pt nanoparticles of a mean diameter of 5 nm (as determined by TEM) after the first, third, and fifth depositions on a gold substrate. We see a low-angle peak with a  $d$ -spacing of 7.2 nm corresponding to the center-to-center distance between two adjacent particles in the array. XRD patterns of such lattices obtained from the deposition of Pt or Au nanoparticles of different sizes reveal that the  $d$ -spacing of the low-angle feature increases with the mean diameter of the nanoparticle as shown in the inset of Figure 1. The intercept on the  $y$ -axis ( $\sim 2$  nm) approximately gives the spacing between two adjacent particles.

A scanning tunneling microscopic study of a layer of 5 nm Pt particles obtained after the first deposition shows regular arrays of nanoparticles extending over 300 nm which corresponds to the size of a typical flat terrace of the substrate. Imaging at lower scan size of  $\sim 40 \times 40$  nm revealed the nearly regular spacing of 2 nm between the spherical particles of 5 nm diameter (Figure 3). This result corroborates the observations from XRD measurements. STM measurements after the deposition of the second layer also showed the presence of 5 nm Pt particles, although the particles were not as clearly resolvable.

Core-level X-ray photoelectron spectra (XPS) of the lattices formed by the 5 nm particles of Pt on a gold substrate are shown

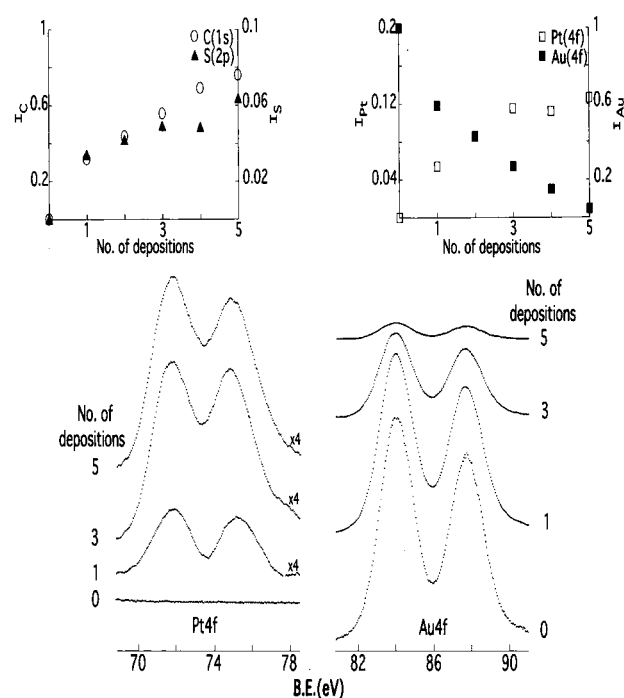


**Figure 4.** X-ray photoelectron spectra in the Pt(4f) and Au(4f) regions for the 5 nm Pt/Au system. Inset shows variations in the Pt(4f) and Au(4f) intensities as well as C(1s) and S(2p) intensities with the number of depositions.

in Figure 4 after the first, third, and fifth depositions. We observe that the intensity of the Pt(4f) feature increases with the number of depositions accompanied by a decrease in the Au(4f) intensity as the substrate gets increasingly shadowed due to the limited escape depth of the photoelectrons. The intensities of the C(1s) and S(2p) levels of the dithiol (at 285.0 and 163.6 eV, respectively) also increase with the increasing number of depositions. We have also carried out similar XPS measurements on lattices formed by 1.5 nm Pt nanoparticles and obtained similar results. XPS measurements on the superlattices formed by 6 nm Au particles on a Ag substrate showed an increase in the Au(4f) intensity accompanied by an increase in the C(1s) and S(2p) intensities due to the dithiol, with the increasing number of depositions. The Ag(3d) intensity decreases with increasing number of depositions as expected. The observed variation of the relevant core-level intensities with successive depositions is clearly indicative of superlattice formation as a result of layer-by-layer deposition. We have estimated the metal coverage after each deposition by employing the Seah–Dench formula<sup>10</sup> for metal overlayers. The plot of metal coverage versus the number of depositions gave a slope close to unity until the third deposition and increased thereafter, suggesting that we have indeed accomplished layer-by-layer deposition of the metal nanoparticles.

We have investigated the formation of a bimetallic superlattice by alternative depositions of 6 nm Au particles and 5 nm Pt particles on a Ag substrate, the particulate layers being separated by decanedithiol molecules. In Figure 5, we show the core-level spectra in the Ag(3d), Au(4f), and Pt(4f) regions. There is a decrease in the intensity of Ag(3d) with successive depositions, while the Au(4f) intensity appears after the first deposition and decreases after the deposition of Pt nanoparticles in the second layer. This experiment provides further proof for the formation of superlattices of arrays of metal nanoparticles by the technique employed by us.

He–I ultraviolet photoelectron spectra of the metal nanoparticles layers were recorded after each deposition. After the

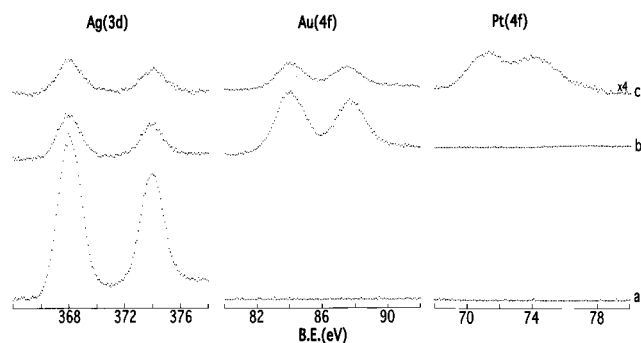


**Figure 5.** X-ray photoelectron spectra in the Ag(3d), Au(4f), and Pt(4f) regions for the Pt/Au/Ag system: (a) clean Ag substrate, (b) after the deposition of the 6 nm Au particles in the first layer, and (c) after the deposition of the 5 nm Pt particles in the second layer.

deposition of the first layer of 1.5 nm Pt nanoparticles, there were no features due to the dithiol-covered Au surface in the spectrum. Instead, there was a distinct feature at 3.5 eV but without the sharp increase in intensity at 0.5 eV found in the bulk Pt. There was a negligible density of states at the Fermi level. These features in the He-I spectra were found up to the fifth deposition. When the diameter of the Pt nanoparticles was larger (5 nm or more), features akin to those of bulk Pt could be seen in the He-I spectrum. The He-I spectra of layers of Au nanoparticles deposited on a Ag substrate showed general characteristics similar to those described for the Pt nanoparticles.

We have been able to prepare heterostructures consisting of alternate layers of semiconductor and metal nanoparticles. For this purpose, we first deposited a layer of 5 nm Pt nanoparticles on a dithiol-covered Au substrate, followed by immersion in dithiol solution, rinsing in toluene, and drying in air. It was then dipped into an inverse micellar solution of AOT (sodium bis(2-ethylhexyl)sulfosuccinate)/*n*-heptane/water containing CdS nanoparticles (2.4 nm) for 12 h in order to obtain a CdS–Pt heterostructure (Figure 1). The excess AOT present on the CdS layer was removed by repeatedly rinsing in *n*-heptane and drying in air. We show XPS evidence for the formation of the heterostructure in Figure 6. The intensity of the Au(4f) core level from the substrate decreases with each deposition. We also see that the core-level intensity in the Pt(4f) region decreases after the deposition of the CdS nanoparticles. The order of deposition of the Pt and CdS particle could be readily reversed to obtain a Pt–CdS–Pt-type heterostructure (Figure 1).

After we completed the present study, our attention was drawn to a recent paper of Brust et al.<sup>11</sup> who reported the formation of multilayers of Au nanoparticles using dithiols. These workers have confirmed layer-by-layer deposition of the Au nanoparticles by employing UV–vis spectroscopy and ellipsometry. They do

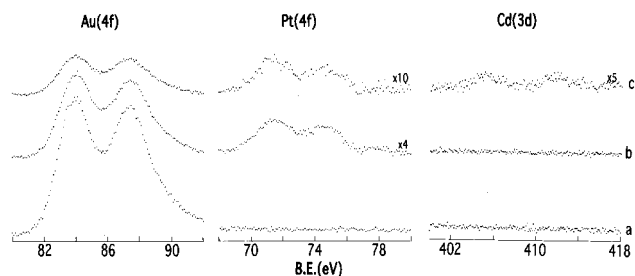


**Figure 6.** X-ray photoelectron spectra in the Cd(3d), Pt(4f), and Au(4f) regions for the CdS/Pt/Au system: (a) clean Au substrate, (b) after the deposition of the 5 nm Pt particles in the first layer, and (c) after the deposition of the 2.4 nm CdS particles in the second layer.

not, however, provide spectrochemical analysis in support of this result. By and large, the results of Brust et al. are in line with the findings of our study, although the techniques employed and the systems studied are different. Noteworthy features of the present study are the use of the dithiol C(1s) and S(2p) intensities along with the intensities of the metal core levels to establish the occurrence of layer-by-layer deposition of Au as well as Pt nanoparticles of different sizes. Deposition of bimetallic layers and metal–semiconductor layers is another aspect worthy of note.

**Acknowledgment.** The authors thank the Department of Science and Technology, Government of India, for support of this research.

## References and Notes

- (1) Colvin, V. L.; Schlamp, M. C.; Alivisatos, A. P. *Nature* **1994**, 370, 354.
- (2) Murray, C. B.; Kagan, C. R.; Bawendi, M. G. *Science* **1996**, 270, 1335.
- (3) Nakanishi, T.; Ohtani, B.; Uosaki, K. *J. Phys. Chem.* **1998**, B102, 1571.
- (4) Brust, M.; Etchenique, R.; Calvo, E. J.; Gordillo, G. J. *Chem. Commun.* **1996**, 1949.
- (5) Alivisatos, A. P.; Johnson, K. P.; Peng, X.; Wilson, T. E.; Loweth, C. J.; Burchez, M. P., Jr.; Schultz, P. G. *Nature* **1996**, 382, 609.
- (6) Hornyak, G. L.; Kröll, M.; Pugin, R.; Sawitowski, T.; Schmid, G.; Bovin, J.-O.; Karsson, G.; Hofmeister, H.; Hopfe, S. *Chem. Eur. J.* **1997**, 3, 1951.
- (7) Andres, R. P.; Beilefeld, J. D.; Henderson, J. I.; Janes, D. B.; Kolagunta, V. R.; Kubaik, C. P.; Mahoney, W. J.; Osifchin, R. G. *Science* **1996**, 273, 1960.
- (8) Vijaya Sarathy, K.; Raina, G.; Yadav, R. T.; Kulkarni, G. U.; Rao, C. N. R. *J. Phys. Chem.* **1997**, B101, 9876.
- (9) Whetten, R. L.; Khoury, J. L.; Alvarez, M. M.; Murthy, S.; Vezmar, I.; Wang, Z.; Stephens, P. W.; Cleveland, C. L.; Luedtke, W. D.; Landmann, U. *Adv. Mater.* **1996**, 8, 428.
- (10) Seah, M. P.; Dench, W. A. *Surf. Interface Anal.* **1979**, 1, 2.
- (11) Brust, M.; Bethell, D.; Kiely, C. J.; Schiffrin, D. J. *Langmuir* **1998**, 14, 5425.